Sensors & Actuators: B. Chemical 394 (2023) 134364

Contents lists available at ScienceDirect

Sensors and Actuators: B. Chemical

journal homepage: www.elsevier.com/locate/snb

Monitoring disease-implicated hydrogen sulfide in blood using a facile deproteinization-based electrochemiluminescence chemosensor system

Yecheol Bak [a,b], Tikum Florence Anjong [a], Jihwan Park [a,c], Sang Hyeon Jeon [d], Jihwan Kim [a,c], Kangwon Lee [b,*], Iksoo Shin [d,*], Sehoon Kim [a,c,**]

[a] Chemical and Biological Integrative Research Center, Korea Institute of Science and Technology (KIST), 02792 Seoul, Republic of Korea
[b] Program in Applied Bioengineering, Graduate School of Convergence Science and Technology, Seoul National University, 08826 Seoul, Republic of Korea
[c] KU-KIST Graduate School of Converging Science and Technology, Korea University, 02841 Seoul, Republic of Korea
[d] Department of Chemistry, College of Natural Science, Soongsil University, 156743 Seoul, Republic of Korea

ARTICLE INFO

Keywords:
Electrochmiluminescence
Chemosensor
Hydrogen sulfide
Small molecule biomarker
Type 1 diabetes

ABSTRACT

Hydrogen sulfide (H_2S), an antioxidant and cell signaling molecule, plays a critical role in redox reactions in the biological system, and its imbalances in blood levels have been implicated in various diseases. Here, we demonstrate a novel chemosensor-based "turn-on" electrochemiluminescence (ECL) system for the selective and sensitive detection of H_2S in a type 1 diabetes rat model. Our luminogenic chemosensor (**Probe**) is a redox-stable cyclometalating iridium (III) complex with emission-quenching 2,4-dinitrophenyl ether (DNP) that shows a significant enhancement in emission intensity upon cleavage of DNP by selective reaction towards H_2S. To achieve robust and reliable ECL emission of **Probe** for biological analysis, we developed a facile deproteinization protocol based on organic solvent-induced protein precipitation/syringe filtration that eliminates uncontrolled protein adsorption on the electrode surface from protein-rich biological samples. Our deproteinization-assisted ECL chemosensor system showed effectiveness in detecting disease-associated H_2S levels in biological media with a linear response in the range of 0–250 μM (R^2: 0.992). It enables reliable *in vitro* monitoring of H_2S level changes in blood samples of a type 1 diabetes rat model ($P = 0.0296$). This strategy to integrate chemosensor-based ECL and facile deproteinization protocol provides a sensitive and rapid disease-monitoring platform for detecting small-molecule biomarkers.

1. Introduction

Electrochemiluminescence (ECL) is a light emission generated by a luminophore near an electrode through electronic excitation following a sequence of electrochemical reactions. Unlike traditional fluorescence techniques, ECL does not require external photoexcitation, allowing for the elimination of autofluorescence background from biological samples and enabling high sensitivity with minimal sample volumes required for measurement (typically >50 μL). Despite its potential, practical applications of ECL with real biological samples are challenging. The presence of abundant proteins in clinical and preclinical samples can nonspecifically passivate the electrode surface in the ECL cell and interfere with electrochemical reactions [1–3]. Deproteinization processes, such as a washing step in the ECL sandwich immunoassay, are required to remove background proteins and selectively capture the target analyte [4,5]. The ECL sandwich immunoassay has been successfully applied to clinical diagnosis [6], but its reliance on antibody recognition limits its ability to detect small-molecule biomarkers such as heavy metals, hormones, and metabolites that play a crucial role in disease progression. An alternative approach, chemosensor-based "turn-on" ECL, is gaining interest in the selective detection of small-molecule analytes [7–9]. However, this format is yet to be validated with protein-rich biological samples. To address these challenges, we developed a "turn-on" chemosensor-based ECL system with a facile deproteinization protocol for selective and sensitive detection of reactive metabolites in blood specimens from animal disease models.

Hydrogen sulfide (H_2S) is a high disease-implicated small-molecule metabolite produced in the body through the degradation of cysteine or

* Corresponding authors.
** Corresponding author at: Chemical and Biological Integrative Research Center, Korea Institute of Science and Technology (KIST), 02792 Seoul, Republic of Korea.
E-mail addresses: kangwonlee@snu.ac.kr (K. Lee), extant@ssu.ac.kr (I. Shin), sehoonkim@kist.re.kr (S. Kim).

https://doi.org/10.1016/j.snb.2023.134364
Received 17 April 2023; Received in revised form 25 July 2023; Accepted 25 July 2023
Available online 31 July 2023

homocysteine by cystathionine γ-lyase or cystathionine β-synthase [10]. It acts as a gasotransmitter in a range of biological processes, including protein post-translation modification, neuronal transmission, and smooth muscle relaxation [11,12]. Recent research has linked imbalances in blood H_2S levels with various diseases, including Alzheimer's disease, diabetes, cardiovascular diseases, and lung diseases [13–16]. This highlights the significance of sensitive H_2S detection in blood for early disease diagnosis and monitoring. Over the years, several methods such as methylene blue method, metal-induced sulfide precipitation, monobromobimane (MBB) method, gas chromatography, gas colorimetric, and electrochemical assays [17–19] have been used to detect H_2S but most of these techniques are very costly, time-consuming and complex to operate. Therefore, it is imperative to develop techniques that are easy to use and very time efficient for the detection of H_2S.

In recent years, fluorescent sensing and imaging have become one of the most prominent ways for *in vivo* and *in vitro* detection of ions and biomolecules. Several fluorescent probes based on different mechanisms such as reduction of azide to amine, trapping of H_2S through nucleophilic addition, copper sulfide precipitation, and thiolysis of dinitrophenyl ether by H_2S [20–25] have been reported for the selective detection of H_2S. Despite the growth in the number of fluorescent probes reported for H_2S, very few luminescent transition metal complexes have been used for the detection of H_2S. Compared to fluorescent probes, transition metal-based ECL probes such as iridium, ruthenium, and osmium complexes have attractive photophysical properties such as high quantum yield, high photostability, and large stoke shift which is beneficial in enhancing the sensitivity of probe in biosensing [26–34]. In this regard, we employed a chemosensor-based ECL system to measure blood H_2S levels. To achieve selective H_2S sensing and robust ECL emission, we designed a redox-stable chemosensor molecule based on a phosphorescent iridium (III) complex (**Probe**). One of its ligands contains two emission-quenching units, i.e., 2, 4-dinitrophenyl ether (DNP), which is selectively removable in response to H_2S, producing a luminogenic, turn-on signal. Our study shows that combining an iridium complex chemosensor with a facile deproteinization process yields a sensitive and reliable ECL monitoring system for diabetes-associated alterations in blood H_2S levels of animal models, offering the potential for use in preclinical and clinical settings.

2. Experiment

2.1. Chemicals

All chemicals were purchased from Sigma-Aldrich (Missouri, USA) and Tokyo Chemical Industry (Tokyo, Japan), and used without further purification. Sodium sulfide (Na_2S) was used to generate H_2S.

2.2. Characterization

Nuclear magnetic resonance (NMR) spectra were collected by using Bruker-400 spectrometry (Bruker, Massachusetts, USA) with TMS as the internal standard. High-resolution mass spectra (HRMS) were collected using Waters Synapt G2 liquid HDMS (Waters, Massachusetts, USA). The UV–vis absorption and phosphorescence spectra were measured at room temperature using Cary 300 UV–vis spectrophotometer (Agilent, California, USA) and PTI QuantaMaster 40 (Horiba, Kyoto, Japan) respectively, with a 1 × 1 cm quartz cuvette. The excitation wavelength for phosphorescence measurement was 350 nm.

2.3. Synthesis of Ir-OH

Ir-OH was synthesized by reacting dichlorotetrakis(2-(2-pyridinyl) phenyl)diiridium(III) ($[Ir(ppy)_2Cl]_2$) with 4,4′-dihydroxy-2,2′-bipyridine ($bpy(OH)_2$), according to the procedure reported in our previous study [35].

2.4. Synthesis of the chemosensor (Probe)

Ir-OH (362 mg, 0.5 mmol) was diluted in 40 mL of dry dichloromethane. To activate the OH group, the solution was mixed with trimethylamine (200 μL) and stirred at room temperature for 30 min 1-Bromo-2,4-nitrobenzene (296 mg, 1.2 mmol) was added to a solution and the reaction mixture was refluxed overnight. After the reaction was completed, the mixture was washed with brine, and the separated organic layer was dried using Mg_2SO_4. The counterion was exchanged by adding an excess amount of sodium perchlorate ($NaClO_4$) to the solution, and the precipitated solid was filtered and washed with distilled water (DW) and ether to afford $Ir(ppy)_2(bpy(2,4\text{-dinitrophenyl ether}))_2$ (**Probe**, Scheme S1, Figs. S1–2). Yield: 75%. Elemental analysis of $C_{44}H_{28}IrN_8O_{10}$: C 51.76%, H 2.76%, Ir 18.83% N 10.98%, O 15.67% HRMS (ESI+, *m/z*): $[M+H]^+$– calcd for $C_{44}H_{28}IrN_8O_{10}$, 1021.1558; found, 1021.1494. HRMS (ESI+, *m/z*): $[M+H]^+$– calcd for $C_{44}H_{28}IrN_8O_{10}$, 1021.1558; found, 1021.1494. 1 H NMR (400 MHz, DMSO-*d6*), δ 6.19 (d, 2 H), 6.90 (t, 2 H), 7.05 (t, 2 H), 7.23 (t, 2 H), 7.55 (dd, 2 H), 7.78 (m, 4 H), 7.84 (m, 2 H), 7.91 (m, 2 H), 7.98 (m, 2 H), 8.28 (m, 2 H), 8.64 (dd, 2 H), 8.79 (d, 2 H), 9.02 (s, 2 H).

2.5. ECL measurement and electrochemical characterization

A disposable screen-printed three-electrode system (Metrohm Dropsens 110, Herisau, Switzerland), composed of a carbon working electrode, a carbon counter electrode, and an Ag wire quasi-reference electrode, was used for the ECL study. The ECL analysis was conducted using a custom-built ECL measurement system (Fig. S3) comprising a photomultiplier (PMT) module (H12386–01, Hamamatsu Photonics, Shizuoka, Japan) and a homemade potentiostat, which enabled synchronized measurement of both voltammetry and ECL signals. The ECL intensity profile was measured during cyclic voltammetry (CV) mode which was carried out in the range of 0–1.4 V at the scan rate of 0.1 V/s. Regarding the ECL molecular sensing of H_2S, the **Probe** solution was mixed with the sample to undergo the selective reaction for a duration of 3 min, and then the resultant solution (50 μL) was applied onto the electrode surface, followed by immediate ECL measurement. For CV analysis, a conventional three-electrode system is used in which a glassy carbon electrode (GCE, working electrode) (3 mm in diameter), Ag/Ag+ electrode (reference electrode), and platinum coil (counter electrode) using CH Instruments 660D Electrochemical Analyzer (CH Instruments, Inc., Texas, USA). The GCE was sonicated in DW/ethanol (1/1, v/v) for 5 min, polished with 0.05 μm alumina, and dried with nitrogen gas. Solutions were prepared with 1 mM of **Probe** and Ir-OH in acetonitrile solution containing 100 mM tetrabutylammonium perchlorate (TBAP) as a supporting electrolyte. 1 v/v % dimethyl sulfoxide (DMSO) was additionally added to Ir-OH. CV was carried out at the scan rate of 0.1 V/s in the range of 0–1.4 V and 0–1.3 V, **Probe,** and Ir-OH, respectively.

2.6. Density functional theory (DFT) calculations

Geometry optimization and time-dependent (TD)-DFT of **Probe** and Ir-OH were carried out by DFT/B3LYP using Gaussian 16 [36]. The LANL2DZ and 6–311 G basis sets were applied to iridium and all other atoms, respectively.

2.7. Type 1 diabetes model

All animal experiments have been approved by the animal care and use committee of the Korea Institute of Science and Technology, and all handling of rats was performed following the institutional regulations. We allow the adaptation period for the rat at least 5 days before starting the experiment. Streptozotocin (STZ)-induced diabetes rat models were prepared with Sprague-Dawley (SD) rats (male, 7 weeks, Orient Bio Inc. Republic of Korea) by intraperitoneal injection of STZ (30 mg/mL/kg)

diluted in 1x PBS (phosphate buffer saline, pH 7.4) during 3 consecutive days [37]. We collected 1 mL of each blood once a week after 8 h fast and check the severity of diabetes by measuring the blood glucose level (Accucheck-Roche, Barozen-Handok, Freestyle-Abbott). *In vitro* ECL experiments were conducted within a day after drawing blood.

3. Results and discussion

3.1. Chemosensor (Probe) design and properties

A phosphorescent iridium (III) complex (Ir-OH) was chosen as a robust ECL luminophore with redox stability to attain an efficient ECL sensing signal. In the design of an H_2S-responsive chemosensor (**Probe**; Scheme S1), each hydroxyl group of Ir-OH was functionalized with 2,4-dinitrophenyl ether (DNP) that serves as a recognition unit for H_2S. DNP is widely used as a detachable receptor for strongly nucleophilic thiol groups [38–41] and is a strong electron acceptor that promotes the photoinduced electron transfer (PET) process, resulting in the luminescence quenching of the sensor. Accordingly, DNP-bearing **Probe** is a luminescence-quenched sensor that transforms into highly luminogenic Ir-OH through loss of DNP upon aromatic nucleophilic substitution reaction with H_2S, which cleaves aryloxy bonds from the **Probe** by thiolysis of the DNP to 2,4-dinitrobenzenethiol (DNBT) (Fig. 1).

When examined in a mixed solvent of 1x PBS (pH 7.4)/acetonitrile (1:2 vol. ratio), **Probe** demonstrated obvious sensor responses to H_2S, as designed (Fig. 2). In the absence of H_2S, **Probe** displayed the typical absorption spectrum of an iridium complex (Fig. 2a), consisting of spin-allowed π–π * intra-ligand transitions of the cyclometalating ligand below 320 nm and d–π * metal-to-ligand charge transfer (MLCT) transitions at 320–450 nm [35,42]. Upon exposure to excess H_2S, a distinct new band appeared at ca. 430 nm, consistent with the known absorption spectrum of DNBT [25], which experimentally implicates its detachment from the **Probe** molecule through the nucleophilic substitution reaction with H_2S (Fig. 1). The proposed sensing mechanism was further evidenced by mass spectrometry of the reaction mixture (**Probe** and excess H_2S), which showed two dominant peaks at m/z 198.9813 and 687.1387, corresponding to DNBT and Ir-OH, respectively (Fig. S4). Fig. 2b displays the H_2S-responsive photoluminescence (PL) spectra, excited at 350 nm, where **Probe** was found to be scarcely emissive as designed with the quenching effect of DNP. When treated with H_2S under the given condition, the PL intensity was increased nearly 10-fold due to the recovery of highly phosphorescent Ir-OH.

We then measured the ECL signal change of **Probe** in response to H_2S by applying it to the electrochemical reaction on a disposable carbon working electrode in the presence of tri-*n*-propylamine (TPrA) as a co-reactant (Fig. 2c). In the co-reactant ECL, both luminophore and co-reactant undergo anodic oxidation at the electrode surface, where the co-reactant produces a strongly reducing radical intermediate that then reduces the oxidized luminophore, creating an excited state (Scheme S2). Similar to the PL response, the ECL signal of **Probe** alone was dim (off-state), but afterward, it was significantly enhanced upon reaction with H_2S (on-state). Notably, the on/off contrast ratio obtained with ECL was estimated to be ~33-fold, which is much higher than that of the PL response (10-fold). The proposed ECL mechanism for the H_2S sensing is summarized as follows:

$$\textbf{Probe} + H_2S \rightarrow \text{Ir-OH} + \text{DNBT} \quad (1)$$

$$\text{Ir-OH} - e^- \rightarrow \text{Ir-OH}^+ \quad (2)$$

$$\text{TPrA} - e^- \rightarrow \text{TPrA}^{\bullet +} \quad (3)$$

$$\text{TPrA}^{\bullet +} - H^+ \rightarrow \text{TPrA}^{\bullet} \quad (4)$$

$$\text{Ir-OH}^+ + \text{TPrA}^{\bullet} \rightarrow \text{Ir-OH}^* + \text{byproduct} \quad (5)$$

$$\text{Ir-OH}^* \rightarrow \text{Ir-OH} + h\nu(\text{ECL}) \quad (6)$$

3.2. Density functional theory (DFT) calculations

The difference in the on/off sensing response between ECL and PL can be attributed to their distinct luminescence mechanisms. To understand the light-emissive excited states of Ir-OH (on-state) and **Probe** (off-state), the molecular energy levels were estimated through thermodynamic simulations at the DFT calculations (Fig. 3) along with electrochemical redox properties under the CV measurements (Fig. S5). The results of the DFT calculations demonstrate that the phosphorescent Ir complex (Ir-OH) has a characteristic MLCT transition. In this complex, electrons in the highest occupied molecular orbital (HOMO) are localized in the iridium center and ppy ligands while they are transferred to the bpy-OH ligand in the lowest unoccupied molecular orbital (LUMO) with a HOMO-LUMO gap of 3.39 eV. In the case of a phosphorescence-quenched **Probe**, one-electron excitation (HOMO → LUMO+4)

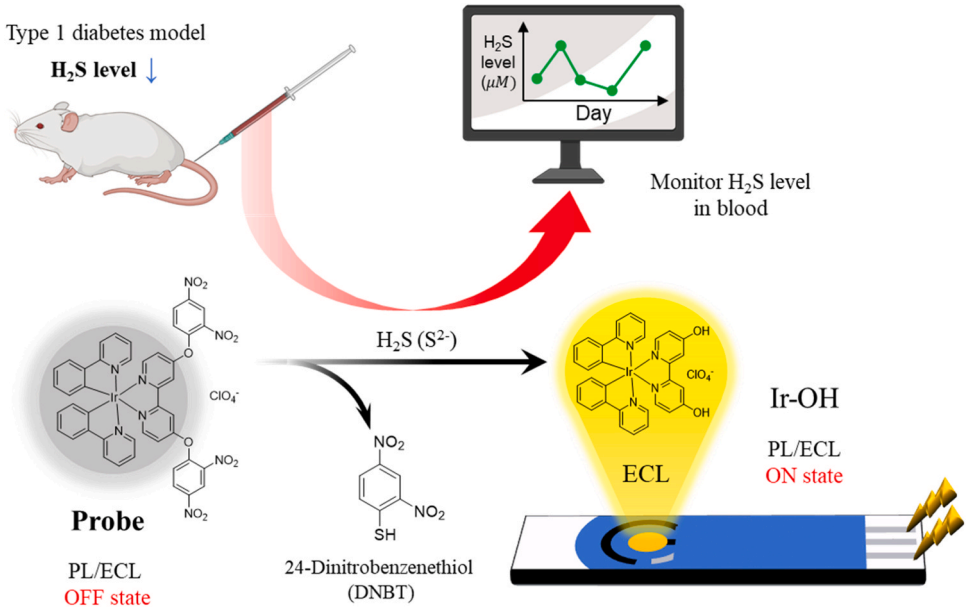

Fig. 1. Overview of the chemosensor (Probe)-based ECL measurement of H_2S in the blood of animal disease models.

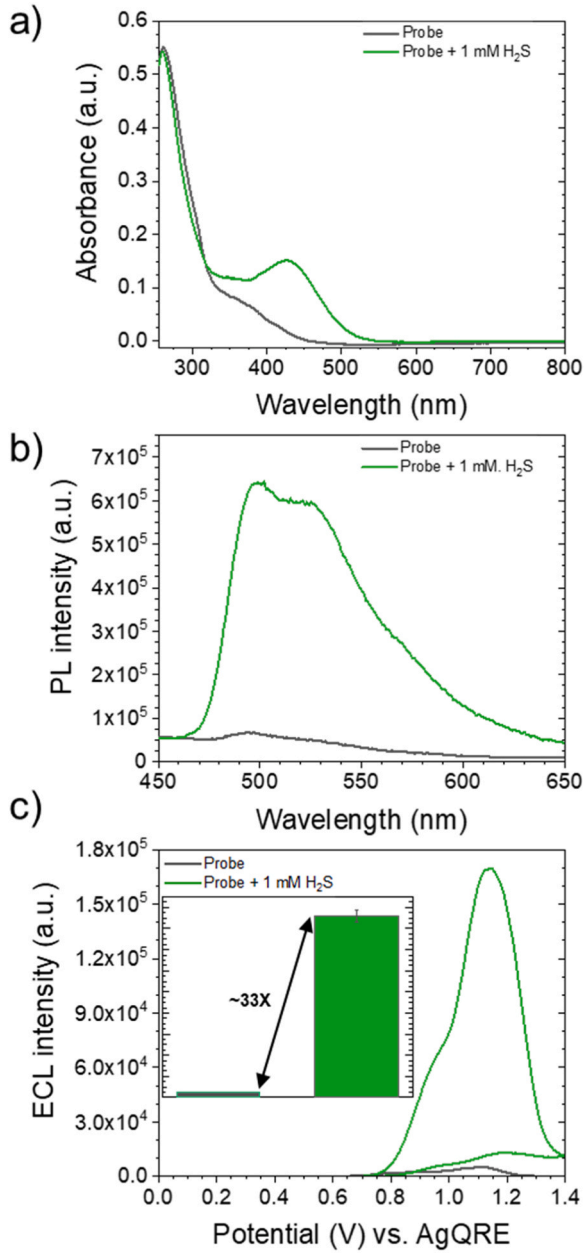

Fig. 2. Chemosensor responses of Probe in the absence and presence of H_2S (1 mM); a) UV-Vis absorption spectra, b) PL spectra, and c) potential-dependent ECL emission profiles under the CV mode (n = 3).

corresponds to the phosphorescent MLCT transition with a gap of 3.23 eV, whereas low-lying LUMO electrons are localized in the electron-accepting quencher units (DNP) attached to bpy-OH via σ bonds (ether linkages). This electronic structure suggests that upon photoexcitation at 350 nm, one electron is excited from HOMO to LUMO+ 4 and spontaneously transferred to σ bond-separated DNP in the energetically favored LUMO, producing a non-emissive charge-separated state via a PET mechanism (HOMO → LUMO+4 → LUMO). This dominant excited-state decay pathway explains the observed phosphorescence quenching. However, it should be noted that while the quenching effect of DNP is significant, the PL of **Probe** is not completely quenched and is still weakly observable (Fig. 2b), indicating that some portion of the photoexcited **Probe** molecules (HOMO → LUMO+4) decay radiatively (LUMO+4 → HOMO) instead of through PET (LUMO+4 → LUMO). This results in a background PL signal in the off state, reducing the on/off contrast in PL.

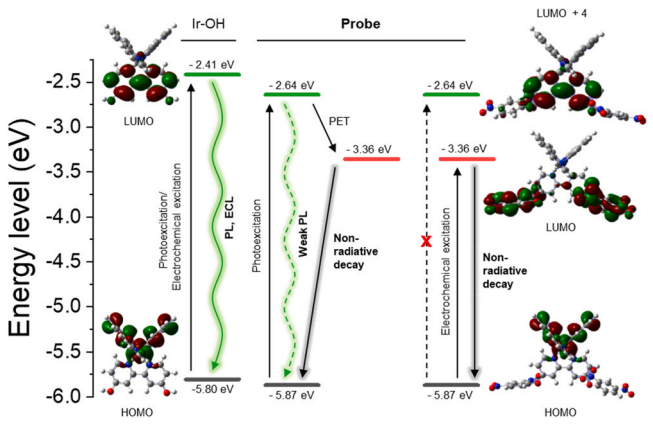

Fig. 3. Energy diagrams of HOMO/LUMO and HOMO/LUMO/LUMO+ 4 orbitals of Ir-OH and Probe, respectively, calculated at the DFT level using a B3LYP functional.

In the mechanism of ECL, an electrochemical redox reaction creates an exciton by oxidizing and reducing the HOMO and the LUMO of a luminophore, respectively (Fig. 3). Unlike photoexcitation, the ECL process directly accesses the non-emissive charge-separated state (HOMO → LUMO) in **Probe**, bypassing the LUMO+ 4 state. This means that the chance of radiative decay in **Probe** (LUMO+4 → HOMO) is minimized and the background signal in the off state is reduced, leading to a higher on/off contrast compared to the PL response.

3.3. Electrochemical analysis

CV was performed to investigate the electrochemical behavior of **Probe** and Ir-OH, and the electrochemical values were calculated based on the CV results over the range from 0 to 1.4 V (Fig. S5, Table S1). For Ir-OH, we observed a quasi-reversible oxidation process from Ir(III) to Ir (IV) at $E_{1/2} = 0.86$ V, which corresponds to the HOMO level of Ir-OH. On the other hand, **Probe** exhibited an irreversible oxidation peak at around 0.73 V, followed by a quasi-reversible process at 0.95 V ($E_{1/2}$) corresponding to the electrochemical conversion between Ir(III) and Ir(IV). The former peak is presumably due to the oxidation of the -O-DNP branch connected to the auxiliary ligand. By comparing the $E_{1/2}$ values of **Probe** and Ir-OH, the oxidation potential of **Probe** was found to be 0.09 V more positive than that of Ir-OH, indicating that the HOMO level of **Probe** is stabilized by 0.09 eV through the attachment of -O-DNP to the auxiliary ligands. This observation is analogous to our previous DFT calculations.

Effective ECL emission requires electrochemical reversibility of a luminophore, which ensures the stability of the luminophore during oxidation and its ability to be fully re-reduced. Key parameters used to estimate electrochemical reversibility include ΔE_{pp} and I_{pc}/I_{pa}, with an ideal value of 59 mV and 1.00, respectively, according to the Nernst equation [43]. In the cyclic voltammogram of Ir-OH (Fig. S5), ΔE_{pp} and I_{pc}/I_{pa} are observed to be close to the ideal values (64 mV and 0.70, respectively), affirming the potential of Ir-OH as a redox-stable ECL luminophore satisfying quasi-reversible electrochemical oxidation for effective ECL emission.

3.4. Deproteinization protocol

Compatibility with protein-rich biological samples is crucial for the reliability and reproducibility of ECL detection, as nonspecific protein deposition on the electrode can interfere with the sensitivity and accuracy of the results. Despite various attempts to deproteinize biological samples for ECL analysis, including centrifugation, antifouling coating on the electrode, use of internal standards, and simple dilution [44,45], most of these methods are inefficient or time-consuming, making them

unsuitable for point-of-care testing (POCT) and/or for monitoring short-lived reactive metabolites such as H_2S (few sec ~ min) [14]. To address this issue, we developed a rapid and efficient deproteinization protocol based on organic solvent-induced protein precipitation/syringe filtration and applied it to the ECL chemosensing of H_2S in blood samples from animal models (Fig. 4). In a general protocol, 200 μL of 100 μM **Probe** in DMSO is mixed with same volume of plasma (or other biological media) and subjected to a chemosensing reaction with H_2S therein, which was observed to be completed in 3 min (Fig. S6). Protein precipitation is then induced by adding acetonitrile (900 μL) to the reaction mixture, and the precipitates are removed by syringe filtration with a highly protein-adsorbing 100 nm nylon filter. 650 μL of the resulting filtrate is further mixed with ECL additives dissolved in 1x PBS (pH 7.4)/acetonitrile to form a final measurement solution of 1 mL (aqueous/organic volume ratio of 1/2) containing 10 mM TPrA (co-reactant), 100 mM tetrabutylammonium perchlorate (TBAP, supporting electrolyte) and 10 μM **Probe**. Only 50 μL of the final solution was used for ECL measurement. The entire procedure, comprising deproteinization, the reaction between **Probe** and analyte, and ECL analysis, could be completed within 7 min. It turned out that the ECL performance could be greatly improved by this protocol (Fig. S7). Even with 10% fetal bovine serum (FBS), the ECL signal showed huge fluctuation (S/N ratio=3.6, Fig. S7a) owing to uncontrolled protein deposition, whereas it was significantly stabilized with improved reproducibility (S/N ratio=45.9, Fig. S7b) and enhanced the sensitivity 2.2-folds after deproteinization (Fig. S7c). Moreover, 10 μM of **Probe** was the most optimal concentration as a final concentration, considering its highest S/N ratio and the concentration of H_2S presented in the body.

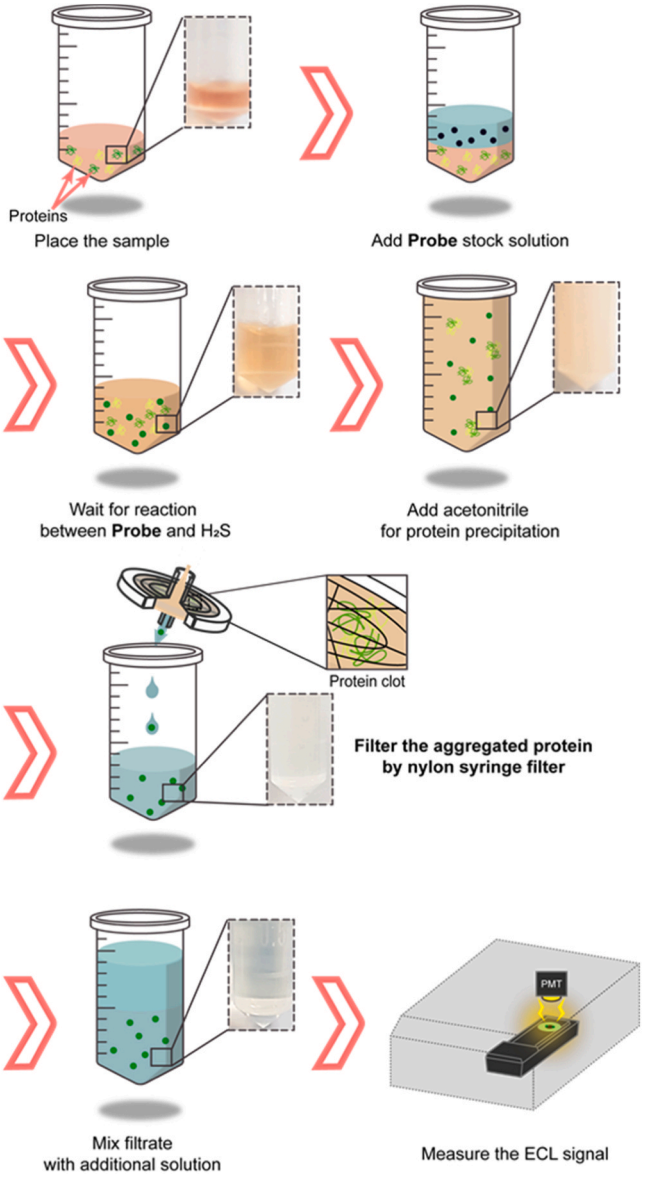

Fig. 4. Sequential protocol of chemosensing and deproteinization for ECL analysis of protein-rich biological samples.

3.5. ECL analysis of H_2S in a protein-rich medium

We assessed the chemosensing performance of **Probe** by ECL in a protein-rich medium (FBS) spiked with a varying amount of H_2S by following the chemosensing/deproteinization protocol described above (Fig. 4). The ECL sensing signal of **Probe** (10 μM) demonstrated a positive correlation with the H_2S concentration, exhibiting a linear response in the range of 0–250 μM (R^2: 0.992) with the limit of detection (LOD, 3.3σ/S) of 7.2 μM, limit of quantification (LOQ, 10σ/S) of 21.6 μM and lower limit of linear range (LLR) of 7.8 μM (Fig. 5a). Within the examined range of H_2S concentrations (0–1 mM), the signal-to-noise ratio (S/N), which was estimated as the mean intensity divided by the standard deviation at each point, was found to be ~25 on average with a minimum of ~15. This indicates a sufficiently high S/N value compared to the S/N criterion (~10) in ELISA which ensures reliable immunoassay [46,47]. Furthermore, the **Probe** displayed high chemo-selectivity in both ECL and PL responses (Fig. 5b and S8). When reacted with various biologically abundant reactive chemical species in FBS, **Probe**

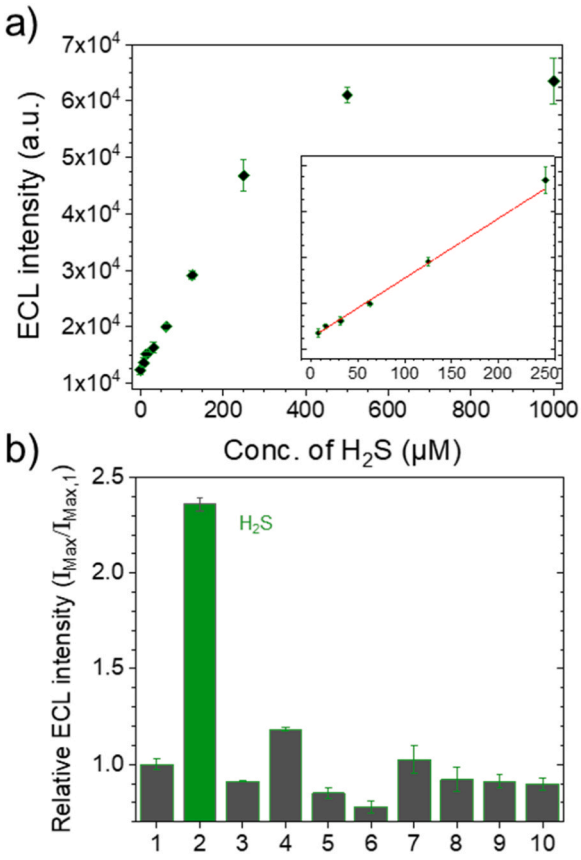

Fig. 5. ECL detection of H_2S spiked in a biological medium (10% FBS) by chemosensing with Probe and deproteinization. a) ECL intensity depending on the concentration of H_2S in the biological medium (n = 3). b) ECL intensity after chemosensing reaction with various analytes (100 μM): (1) Probe only; (2) H_2S; (3) SO_4^-; (4) $S_2O_4^-$; (5) SCN^-; (6) H_2O_2; (7) O_2; (8) cysteine; (9) homocysteine; (10) glutathione reduced (n = 3).

responded specifically to H_2S with a substantial signal recovery. Based on the reported clinical blood level of H_2S in the range of 30–300 μM [12,48], our ECL chemosensor system is anticipated to reliably monitor disease-implicated H_2S alterations by virtue of the deproteinization-assisted stabilization of ECL measurements.

3.6. Monitoring the blood H_2S level in a type 1 diabetes rat model

Finally, we applied our deproteinization-assisted ECL chemosensor system to *in vitro* disease monitoring using preclinical blood samples from animal models. As a model chronic disease, type 1 diabetes mellitus was induced in rats by streptozotocin injection, and blood samples were drawn to monitor the blood levels of glucose and H_2S. As shown in Fig. 6a, the diabetes group (n = 3) showed a gradual increase in blood glucose level over time, confirming the successful induction of type 1 diabetes with the destruction of pancreatic β cells by streptozotocin. For H_2S measurement, the blood samples were processed using our deproteinization protocol (Fig. 4) and subjected to ECL chemosensing with **Probe**. It was observed that at all examined time points, the plasma ECL signal was statistically low in the diabetes group compared to non-diabetic control rats (n = 3) (Fig. 6b). With an inverse correlation to the blood glucose alteration, the ECL tendency suggests that H_2S may be involved in the pathogenesis of diabetes and is in agreement with the results of the previous study [48]. This finding is also consistent with the known fact that H_2S levels in diabetes patients drop in blood but rise in organs such as the pancreas or liver, making it a potential blood biomarker for *in vitro* monitoring of diabetes [15,49]. It also met statistical significance by calculating the P value (P = 0.0296). Detailed ECL values of each sample are shown in Table S2. To the best of our knowledge, this is the first report to demonstrate the potential of an ECL chemosensor for rapid and sensitive disease monitoring with real preclinical blood samples.

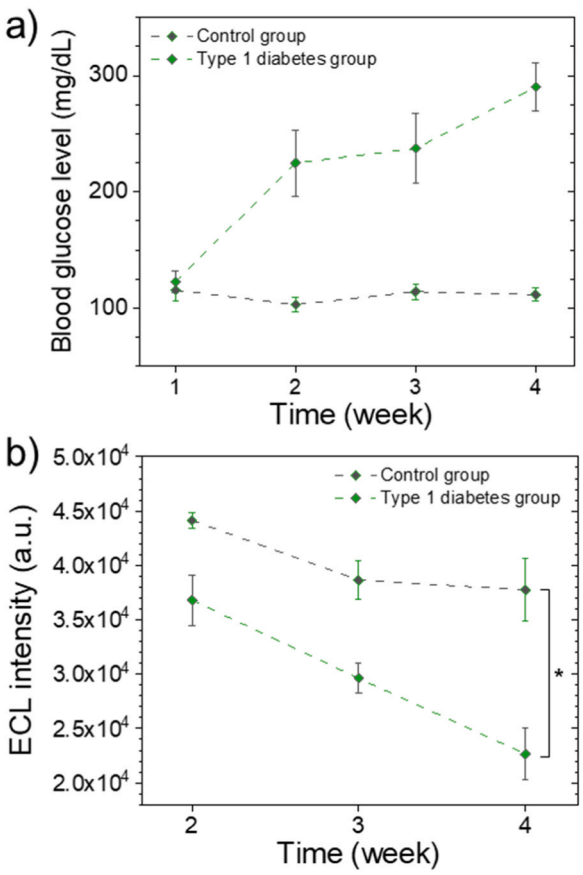

Fig. 6. a) Blood glucose level and b) corresponding ECL chemosensing intensity of Probe showing the H_2S level in the blood collected from control (n = 3) and the rat model of type 1 diabetes (n = 3). *Note: P value for ECL intensity at 4 week corrected two-sample t-test assuming equal variances.* * : P < 0.05.

4. Conclusions

In conclusion, we have successfully developed a chemosensor-based ECL disease-monitoring system by integrating a redox-stable metal complex-based chemosensor (**Probe**) and a simple deproteinization protocol. **Probe** was specifically designed and synthesized to react with H_2S in blood to generate a "turn-on" ECL signal whose intensity is proportional to the H_2S concentration. Experiments demonstrated that **Probe** exhibits excellent selectivity and sensitivity towards H_2S in both PL and ECL, even in protein-rich biological media. To enable the application of ECL for preclinical/clinical analysis, we also developed a rapid and efficient deproteinization protocol based on organic solvent-induced protein precipitation/syringe filtration. By applying this protocol to biological media, the interference by nonspecific adsorption of proteins on the electrode could be effectively removed to achieve robust and reproducible ECL signals. We have shown that our deproteinization-based ECL chemosensor system can reliably monitor changes in blood H_2S levels in a rat model of type 1 diabetes. We believe that this strategy can be utilized to develop a highly sensitive *in vitro* diagnostic platform for detecting a wide range of small-molecule biomarkers that cannot be detected by conventional ECL sandwich immunoassays. Overall, our work provides a promising approach to developing a reliable and rapid disease-monitoring system for early diagnosis and timely intervention in various diseases.

CRediT authorship contribution statement

Yechoel Bak and **Tikum Florence Anjong** contributed equally to this work. **Tikum Florence Anjong** synthesized **Probe**. **Yecheol Bak** and **Jihwan Kim** conducted all photophysical property measurements. Disease animal model preparation and all biological assay were designed and executed by **Yecheol Bak**, **Jihwan Kim**, and **Jihwan Park**. DFT calculation was conducted by **Yecheol Bak**. **Sang Hyeon Jeon** conducted an electrochemical analysis. The overall project was designed and supervised by **Kangwon Lee**, **Iksoo Shin**, and **Sehoon Kim**. The first draft of the manuscript was prepared mainly by **Yecheol Bak** and **Sehoon Kim**, and the final manuscript was revised through the contributions of all authors. All authors have given approval to the final version of the manuscript.

Declaration of Competing Interest

The authors declare that they have no known competing financial interests or personal relationships that could have appeared to influence the work reported in this paper.

Data Availability

Data will be made available on request.

Acknowledgements

Jun-Seok Lee (College of Pharmacology, Korea University) and Youngmin You (Division of Chemical Engineering and Materials Science, Ewha Womans University) were advised on the DFT calculation. This work was supported by grants from the National Research Foundation of Korea (2017M3A9D8029942, 2021R1A2C2005418, and 2022M3H4A1A03076638), the Korea Health Industry Development Institute (HW20C2104), and the KIST intramural program.

Appendix A. Supporting information

Supplementary data associated with this article can be found in the online version at doi:10.1016/j.snb.2023.134364.

References

[1] J. Contreras-Naranjo, O. Aguilar, Suppressing non-specific binding of proteins onto electrode surfaces in the development of electrochemical immunosensors, Biosensors 9 (2019) 15.
[2] A.J. Downard, A.D. Roddick, Protein adsorption at glassy carbon electrodes: the effect of covalently bound surface groups, Electroanalysis 7 (1995) 376–378.
[3] S.E. Moulton, J.N. Barisci, A. Bath, R. Stella, G.G. Wallace, Investigation of protein adsorption and electrochemical behavior at a gold electrode, J. Colloid Interface Sci. 261 (2003) 312–319.
[4] B. Babamiri, D. Bahari, A. Salimi, Highly sensitive bioaffinity electrochemiluminescence sensors: recent advances and future directions, Biosens. Bioelectron. 142 (2019), 111530.
[5] A. Abdussalam, G. Xu, Recent advances in electrochemiluminescence luminophores, Anal. Bioanal. Chem. 414 (2022) 131–146.
[6] Z. Guo, T. Hao, S. Du, B. Chen, Z. Wang, X. Li, et al., Multiplex electrochemiluminescence immunoassay of two tumor markers using multicolor quantum dots as labels and graphene as conducting bridge, Biosens. Bioelectron. 44 (2013) 101–107.
[7] C. Ma, W. Wu, Y. Peng, M.X. Wang, G. Chen, Z. Chen, et al., A spectral shift-based electrochemiluminescence sensor for hydrogen sulfide, Anal. Chem. 90 (2018) 1334–1339.
[8] C.K.P. Truong, T.D.D. Nguyen, I.-S. Shin, Electrochemiluminescent chemosensors for clinical applications: a review, BioChip J. 13 (2019) 203–216.
[9] Y.H. Seo, T. Kim, C.K.P. Truong, H.S. No, J.-I. Hong, I.-S. Shin, Electrochemiluminescent "turn-on" chemosensor based on the selective recognition binding kinetics with glutathione, Sens. Actuators B: Chem. 357 (2022).
[10] T.V. Mishanina, M. Libiad, R. Banerjee, Biogenesis of reactive sulfur species for signaling by hydrogen sulfide oxidation pathways, Nat. Chem. Biol. 11 (2015) 457–464.
[11] L. Li, P. Rose, P.K. Moore, Hydrogen sulfide and cell signaling, Annu. Rev. Pharmacol. Toxicol. 51 (2011) 169–187.
[12] K.R. Olson, Is hydrogen sulfide a circulating "gasotransmitter" in vertebrate blood? Biochim. Biophys. Acta - Bioenerg. 1787 (2009) 856–863.
[13] B.D. Paul, S.H. Snyder, Gasotransmitter hydrogen sulfide signaling in neuronal health and disease, Biochem. Pharmacol. 149 (2018) 101–109.
[14] D.J. Polhemus, D.J. Lefer, Emergence of hydrogen sulfide as an endogenous gaseous signaling molecule in cardiovascular disease, Circ. Res. 114 (2014) 730–737.
[15] C. Szabo, Roles of hydrogen sulfide in the pathogenesis of diabetes mellitus and its complications, Antioxid. Redox Signal. 17 (2012) 68–80.
[16] Q. Xiao, J. Ying, L. Xiang, C. Zhang, The biologic effect of hydrogen sulfide and its function in various diseases, Medicine 97 (2018).
[17] Q. Chen, P. Xing, Y. Xu, H. Li, S. Sun, A selective fluorescent sensor for fast detection of hydrogen sulfide in red wine, Chin. J. Chem. Eng. 35 (2017) 477–482.
[18] Y. Zhao, X. Zhu, H. Kan, W. Wang, B. Zhu, B. Du, et al., A highly selective colorimetric chemodosimeter for fast and quantitative detection of hydrogen sulfide, Analyst 137 (2012) 5576.
[19] J.E. Doeller, T.S. Isbell, G. Benavides, J. Koenitzer, H. Patel, R.P. Patel, et al., Polarographic measurement of hydrogen sulfide production and consumption by mammalian tissues, Anal. Biochem. 341 (2005) 40–51.
[20] L. Zhou, Y. Chen, B. Shao, J. Cheng, X. Li, Recent advances of small-molecule fluorescent probes for detecting biological hydrogen sulfide, Front. Chem. Sci. Eng. (2021).
[21] R. Wang, X. Gu, Q. Li, J. Gao, B. Shi, G. Xu, et al., Aggregation enhanced responsiveness of rationally designed probes to hydrogen sulfide for targeted cancer imaging, J. Am. Chem. Soc. 142 (2020) 15084–15090.
[22] A.K. Alyan, R.S. Hanafi, M.Z. Gad, Point-of-care testing and optimization of sample treatment for fluorometric determination of hydrogen sulphide in plasma of cardiovascular patients, J. Adv. Res. 27 (2021) 1–10.
[23] H. Peng, Y. Cheng, C. Dai, A.L. King, B.L. Predmore, D.J. Lefer, et al., A fluorescent probe for fast and quantitative detection of hydrogen sulfide in blood, Angew. Chem. Int. Ed. 50 (2011) 9672–9675.
[24] Y. Qian, L. Zhang, S. Ding, X. Deng, C. He, X.E. Zheng, et al., A fluorescent probe for rapid detection of hydrogen sulfide in blood plasma and brain tissues in mice, Chem. Sci. 3 (2012) 2920.
[25] W. Zhang, J. Kang, P. Li, H. Wang, B. Tang, Dual signaling molecule sensor for rapid detection of hydrogen sulfide based on modified tetraphenylethylene, Anal. Chem. 87 (2015) 8964–8969.
[26] S. Sprouse, K.A. King, P.J. Spellane, R.J. Watts, Photophysical effects of metal-carbon.sigma. bonds in ortho-metalated complexes of iridium(III) and rhodium (III), J. Am. Chem. Soc. 106 (1984) 6647–6653.
[27] H.D. Abruña, Electrochemiluminescence of osmium complexes: spectral, electrochemical, and mechanistic studies, J. Electrochem. Soc. 132 (1985) 842–849.
[28] J.I. Kim, I.-S. Shin, H. Kim, J.-K. Lee, Efficient electrogenerated chemiluminescence from cyclometalated iridium(III) complexes, J. Am. Chem. Soc. 127 (2005) 1614–1615.
[29] K.N. Swanick, S. Ladouceur, E. Zysman-Colman, Z. Ding, Bright electrochemiluminescence of iridium(iii) complexes, Chem. Comm. 48 (2012) 3179.
[30] Y. You, Recent progress on the exploration of the biological utility of cyclometalated iridium(III) complexes, J. Chin. Chem. Soc. 65 (2018) 352–367.
[31] H. Wei, E. Wang, Electrochemiluminescence of tris(2,2′-bipyridyl)ruthenium and its applications in bioanalysis: a review, Luminescence 26 (2011) 77–85.
[32] X. Zhou, D. Zhu, Y. Liao, W. Liu, H. Liu, Z. Ma, et al., Synthesis, labeling and bioanalytical applications of a tris(2,2′-bipyridyl)ruthenium(II)-based electrochemiluminescence probe, Nat. Protoc. 9 (2014) 1146–1159.
[33] A. Kapturkiewicz, Cyclometalated iridium(III) chelates—a new exceptional class of the electrochemiluminescent luminophores, Anal. Bioanal. Chem. 408 (2016) 7013–7033.
[34] Z. Liu, W. Qi, G. Xu, Recent advances in electrochemiluminescence, Chem. Soc. Rev. 44 (2015) 3117–3142.
[35] T.F. Anjong, H. Choi, J. Yoo, Y. Bak, Y. Cho, D. Kim, et al., Multifunction-harnessed afterglow nanosensor for molecular imaging of acute kidney injury in vivo, Small (2022), 2200245.
[36] S. Lee, Y. Lee, K. Kim, S. Heo, D.Y. Jeong, S. Kim, et al., Twist to boost: circumventing quantum yield and dissymmetry factor trade-off in circularly polarized luminescence, Inorg. Chem. 60 (2021) 7738–7752.
[37] M.D. Mythili, R. Vyas, G. Akila, S. Gunasekaran, Effect of streptozotocin on the ultrastructure of rat pancreatic islets, Microsc. Res. Tech. 63 (2004) 274–281.
[38] T. Fang, X.-D. Jiang, C. Sun, Q. Li, BODIPY-based naked-eye fluorescent on-off probe with high selectivity for H2S based on thiolysis of dinitrophenyl ether, Sens. Actuators B: Chem. 290 (2019) 551–557.
[39] Y. Gu, Z. Zhao, G. Niu, R. Zhang, H. Zhang, G.-G. Shan, et al., Ratiometric detection of mitochondrial thiol with a two-photon active AIEgen, ACS Appl. Bio Mater. 2 (2019) 3120–3127.
[40] Z. Huang, S. Ding, D. Yu, F. Huang, G. Feng, Aldehyde group assisted thiolysis of dinitrophenyl ether: a new promising approach for efficient hydrogen sulfide probes, Chem. Comm. 50 (2014) 9185–9187.
[41] J. Zhou, S. Xu, X. Dong, W. Zhao, Q. Zhu, 3,5-dinitropyridin-2-yl as a fast thiol-responsive capping moiety in the development of fluorescent probes of biothiols, Dyes Pigm. 167 (2019) 157–163.
[42] S. Lee, W.-S. Han, Cyclometalated Ir(iii) complexes towards blue-emissive dopant for organic light-emitting diodes: fundamentals of photophysics and designing strategies, Inorg. Chem. Front. 7 (2020) 2396–2422.
[43] C. Sandford, M.A. Edwards, K.J. Klunder, D.P. Hickey, M. Li, K. Barman, et al., A synthetic chemist's guide to electroanalytical tools for studying reaction mechanisms, Chem. Sci. 10 (2019) 6404–6422.
[44] H. Li, N. Arroyo-Currás, D. Kang, F. Ricci, K.W. Plaxco, Dual-reporter drift correction to enhance the performance of electrochemical aptamer-based sensors in whole blood, J. Am. Chem. Soc. 138 (2016) 15809–15812.
[45] Q. Wei, T. Becherer, S. Angioletti-Uberti, J. Dzubiella, C. Wischke, A.T. Neffe, et al., Protein interactions with polymer coatings and biomaterials, Angew. Chem. Int. Ed. 53 (2014) 8004–8031.
[46] M. Nichkova, D. Dosev, A.E. Davies, S.J. Gee, I.M. Kennedy, B.D. Hammock, Quantum dots as reporters in multiplexed immunoassays for biomarkers of exposure to agrochemicals, Anal. Lett. 40 (2007) 1423–1433.
[47] A. Chen, D. Kozak, B.J. Battersby, R.M. Forrest, N. Scholler, N. Urban, et al., Antifouling surface layers for improved signal-to-noise of particle-based immunoassays, Langmuir 25 (2009) 13510–13515.
[48] S.K. Jain, R. Bull, J.L. Rains, P.F. Bass, S.N. Levine, S. Reddy, et al., Low levels of hydrogen sulfide in the blood of diabetes patients and streptozotocin-treated rats causes vascular inflammation? Antioxid. Redox Signal. 12 (2010) 1333–1337.
[49] L. Zhang, X.E. Zheng, F. Zou, Y. Shang, W. Meng, E. Lai, et al., A highly selective and sensitive near-infrared fluorescent probe for imaging of hydrogen sulphide in living cells and mice, Sci. Rep. 6 (2016) 18868.

Yecheol Bak obtained his BS degree in 2014 from the Department of Nanoenergy Engineering, Pusan National University (PNU), Korea. He is currently an integrated Ph.D. candidate in the Program in Applied Bioengineering, at Seoul National University (SNU), Korea, and carrying out his research at the Korea Institute of Science and Technology under the guidance of Professor Kangwon Lee and Professor Sehoon Kim. His research interests are focused on the design and *in vivo/in vitro* application of luminescence probes.

Tikum Florence Anjong received her Ph.D. in inorganic chemistry in 2018, from the Department of Chemistry and Nanoscience at Ewha Womans University. After research experiences as a post-doctor at Ewha Womans University, she joined the Korea Institute of Science and Technology (KIST) in January 2019 as a postdoctoral fellow. She is currently a postdoctoral fellow at the Department of medical imaging at the University of Saskatchewan. Her research interest is the development of radioimmunoconjugate for targeted therapy and the development of in vivo/in vitro probes for bioluminescence and fluorescence applications.

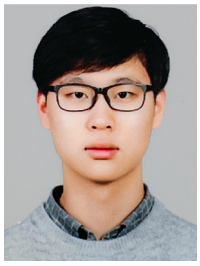

Jihwan Park obtained his BS degree in 2020 from the Department of Biotechnology, Korea University, Korea. He is currently an integrated Ph.D. candidate from the KU-KIST Graduate School of Converging Science and Technology (Korea University, Korea) with Professor Sehoon Kim's research group. His research interests focus on Biochemistry and point-of-care testing (POCT) biomolecular sensors.

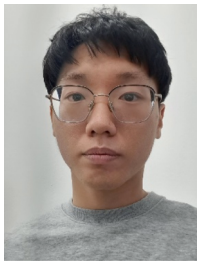

Sang Hyeon Jeon obtained an MS degree in science from the Graduate School of Soongsil University in 2021. He is currently a doctoral student in the Department of Chemistry at Soongsil University and is conducting research under the guidance of Professor Ik-Soo Shin of Soongsil University. His research interests are focused on electrochemistry and electrochemiluminescence and biosensors using them.

Jihwan Kim obtained his MS degree in 2022 from KU-KIST Graduate School of Converging Science and Technology (Korea University, Korea) under the guidance of Professor Sehoon Kim. His research interests are focused on NBIT (Nano Bio Information Technology)

Kangwon Lee received a Ph.D. degree in MSE from the University of Michigan, Ann Arbor. He has further studied cell and tissue engineering at Harvard University as a Postdoctoral Fellow under the supervision of Prof. D. J. Mooney. He was a Senior Research Scientist with the Korea Institute of Science and Technology (KIST) and an Adjunct Associate Professor of biomedical engineering with the University of Science and Technology (UST), South Korea. He is currently an Assistant Professor at the Graduate School of Convergence Science and Technology, Seoul National University (SNU), South Korea. His expertise spans interdisciplinary fields of tissue engineering and biosensors.

Ik-soo Shin obtained his Ph.D. in Electroanalytical Chemistry in 2007, from the College of Natural Sciences at Seoul National University (SNU). After research experiences as a post-doctor at the University of Texas at Austin (UTAUS) and Seoul National University, he joined Soongsil University (SSU) in September 2019. He is currently an associate professor at Soongsil University. His research interest is electrochemistry, electrochemiluminescence, and biosensors using them.

Sehoon Kim received his Ph.D. in Materials Science and Engineering in 2002, from the College of Engineering at Seoul National University (SNU). After research experiences as a post-doctor at the State University of New York at Buffalo (SUNY), he joined the Korea Institute of Science and Technology (KIST) in March 2008. He is currently a Principal Research Scientist and Head of the Center for Theragnosis at KIST. He is also affiliated as Professor at KU-KIST Graduate School of Converging Science and Technology (Korea University) and the Division of Biomedical Engineering, Korea University of Science and Technology (UST). His research interest is the development of advanced drug delivery systems and biophotonic molecular nanoparticles for *in vivo* theranostic applications.